PHYSICAL REVIEW B VOLUME 47, NUMBER 13 1 APRIL 1993-I

Nonlinear transport of vibrational energy in a random molecular chain

A. V. Zolotaryuk,* K. H. Spatschek, and O. Kluth
Institut für Theoretische Physik, Heinrich-Heine-Universität Düsseldorf, D-4000 Düsseldorf, Germany

(Received 30 June 1992)

A generalized model for the nonlinear transport of vibrational energy in a molecular chain is derived. It contains the coupling to both the optical and the acoustic modes of the lattice. The model reduces in simplified situations to the Davydov model or the Holstein model. Reductions to two forms of discrete nonlinear Schrödinger equations are discussed, and the corresponding solitary wave solutions are presented. In general, the molecular chain contains some randomness, which is caused by different physical mechanisms: (i) randomly distributed molecules around the chain, (ii) different masses of the side groups, and (iii) random distributions of the intermolecular distances. The various effects are discussed, and special attention is given to their influences on the transmission coefficient. Besides Anderson localization in the (nearly) linear regime, it is found that solitonlike waves can be excited, which may lead to an anomalous nonlinear convective transport of vibrational energy. This is a very important effect in a random molecular chain.

I. INTRODUCTION

The transfer of vibrational energy in biological systems, such as long chains of hydrogen-bonded peptide groups (PG's), by means of self-trapped mobile states (solitary waves or solitons) was suggested by Davydov and Kyslukha.[1] The idea was to explain how the energy released by hydrolysis of adenosine triphosphate (ATP) can be transported from one end of a protein molecule to the other.[2] The amount of this energy is about 0.422 eV. It is partly stored in the high-frequency intramolecular $C{=}O$ stretching mode (amide-*I* vibrations with frequency about 1665 cm^{-1}). Besides the usual electric dipole-dipole coupling (resonance interaction) between neighboring PG's, which can be described by the standard exciton Hamiltonian, Davydov and Kyslukha have introduced the short-range interaction of amide-*I* vibrations with low-frequency longitudinal acoustic phonons of the molecular chain.[3] The latter coupling is caused by the dependence of the amide-*I* energy on the distances to neighboring left and right molecules (PG's). The linear (in intermolecular relative displacements) expansion term of this dependence leads to the nonlinear exciton-phonon coupling. Then the dispersive effects caused by the resonance interaction are counterbalanced by this nonlinearity resulting in the existence of the dynamically stable so-called Davydov solitons.[4-12] For a comprehensive review and today's status of the theory see Ref. 13.

The main point in the Davydov theory is the self-trapping mechanism originated from the classical works of Landau[14] and Pekar.[15] Based on Pekar's polaron, a simple one-dimensional model for a diatomic molecular crystal has been introduced and studied by Holstein.[16] The model consists of a discrete nonlinear Schrödinger (NLS) equation of the tight-binding form. The wave function describes the probability amplitude of a single excess electron in the conduction band. As was discovered by Scott and co-workers,[17] the Holstein model proved to be very appropriate for the explanation of spectroscopic data measured on crystalline acetanilide, $(\mathrm{CH_3CONHC_6H_5})_x$ or ACN, at low temperatures. In Davydov's model the wave function of the discrete NLS equation describes the self-trapped localized states of the amide-*I* vibrational energy. This self-trapping results from the (nonlinear) coupling of the high-frequency $C{=}O$ stretching mode with low-frequency acoustic modes of this crystal.

In this paper we consider the nonlinear coupling of the amide-*I* high-frequency oscillations with both the acoustic and the (low-frequency) optical modes. If only the first coupling is present, we obtain the Davydov model, whereas, if only the second coupling is present, the Holstein model is found as the limiting case. Besides this generalization, a big part of this paper deals with the influence of a random environment on the excitation and dynamics of possible solitary states. Usually, any chain will be influenced by the environment consisting of molecules randomly distributed around this chain. Besides this type of randomness, irregularities are also caused by the different masses of PG's, including their side groups. Finally, a third type of randomness originates from a possible random distribution of the intermolecular distances involving a random distribution of the intersite coupling constants. When investigating the transport of vibrational energy in a random molecular chain we want to find out whether the Anderson localization[18] occurs also in the nonlinear regime. The Anderson localization means that in scattering experiments the transmission coefficient decays exponentially to zero with increasing scattering lengths. The question is whether this phenomenon will be changed when propagating solitons can be excited.[19] The latter (collective) modes may possess a sufficiently large inertia which could enable the solitons to override the irregularities caused by the randomness. This important problem will be investigated in this paper.

The paper is organized as follows: Since we study a generalization of the Davydov and Holstein models, in Sec. II we combine the acoustic and optical modes and write a general set of three difference-differential equations. In Sec. III we reduce these equations to discrete NLS equations. We also present there the well-known sech-soliton solutions. In Sec. IV we list typical parameter values for both limits, the Davydov and Holstein models. Models for one-quantum dynamics in a random molecular chain are discussed in Sec. V. A particlelike dynamical equation is also derived in that section. Results of numerical scattering experiments in a random chain are shown in Sec. VI. The role of soliton solutions will be shown. Some concluding remarks are outlined in Sec. VII. The paper is supplemented by two appendices. In the first one, the modulational instability of discrete systems is analyzed. In the second one we present the multiparticle generalizations of the previous models for future investigations.

II. A GENERAL NONLINEAR MODEL FOR THE TRANSFER OF THE INTRAMOLECULAR EXCITATION

Let molecules (e.g., peptide groups), in each of which some low-frequency translational and/or rotational motions of atoms take place, be situated along the x axis at sites $x = nl$, with $n = 0, \pm 1, \ldots$ and lattice spacing l. The nearest-neighboring molecules are considered to be coupled (in the simplest case harmonically, "as realized by springs"), so that the equidistant sites $x = nl$ are their equilibrium positions. Besides the intramolecular motions resulting in optical modes, each molecule can move along the x axis as a whole entity. As a result, the longitudinal acoustic mode in the chain will be generated.

Next, each molecule can be found in the excited state. In the case of protein consisting of coupled peptide groups we have the intramolecular high-frequency C=O oscillations (the amide-I excitation mode with a frequency of approximately 1665 cm^{-1}). In this paper, this mode is described quantum-mechanically, whereas the acoustic and optical (low-frequency) modes are treated classically. We present schematically this model chain in Fig. 1. Here, for simplicity of notations, we restrict ourselves to one (low-frequency) optical mode, shown in Fig. 1 by the pair of coupled atoms. For the intramolecular amide-I excitations the exciton Hamiltonian[1] can be used. For our general model it may be written as

$$H = \sum_n [E_n B_n^\dagger B_n - B_n^\dagger (J_{n-1} B_{n-1} + J_n B_{n+1})] , \tag{1}$$

where E_n is the energy of the excited amide-I at the nth molecule (PG) which depends on both, the relative displacements of the nth molecule and its neighbors, as well as on the intramolecular displacements of atoms. J_n is the energy of the resonance dipole-dipole interaction of the excitations at the nth and $(n+1)$th molecules. In a general case it also depends on the relative distance between these molecules. $B_n^\dagger$ and B_n are the operators of creation and annihilation of a quantum of the intramolecular excitation at the nth molecule which satisfy the usual commutation relations

$$[B_n, B_{n'}^\dagger] = \delta_{nn'}, \quad [B_n, B_{n'}] = 0 = [B_n^\dagger, B_{n'}^\dagger] . \tag{2}$$

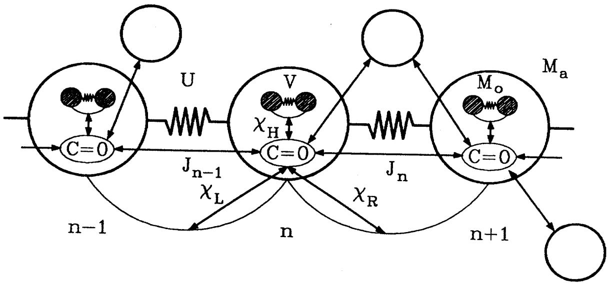

FIG. 1. Schematic representation of the model chain and the environment. Only three molecules of the chain and three molecules of the environment are shown. Inside each molecule the pair of coupled (by the potential V) atoms represents a low-frequency optical mode, and the amide-I mode is shown by the C=O symbols. Double arrows represent interactions.

It is appropriate to expand the quantities E_n and J_n as follows:

$$E_n = E_0 + [\chi_L(\alpha_n - \alpha_{n-1}) + \chi_R(\alpha_{n+1} - \alpha_n) + \chi_H \beta_n] + \cdots , \tag{3}$$

and

$$J_n = J + \chi_J(\alpha_n - \alpha_{n+1}) + \cdots , \tag{4}$$

where E_0 and J are the energy of the excitation in amide-I and the interaction of these excitations at neighboring molecules in the undistorted chain, respectively. The coefficients $\chi_L \geq (\chi_R \geq 0)$ are the constants of the interaction of the intramolecular excitations with the relative displacements of the left (right) molecules. α_n is the displacement of the nth PG from its equilibrium position; $\chi_H \geq 0$ is the constant of the interaction of the excitation amide-I with the intramolecular displacement of atoms β_n (in the nth molecule), the constant χ_J (the sign of which coincides with that of J) describes the degree of decreasing the resonance interaction when the distance between the neighboring molecules is increasing.

Let us start with one quantum of the amide-I excitation in the chain. In this case, the time-dependent wave function for the state of the chain can be represented as[4]

$$|\Psi(t)\rangle = \sum_n \psi_n(t) B_n^\dagger |0\rangle , \tag{5}$$

where $|0\rangle$ is the ground state (the exciton vacuum), and the set of the coefficient functions $\psi_n(t)$ represents the probability amplitude for the excitation quantum to be found at the nth PG. From the normalization condition $\langle \Psi(t) | \Psi(t) \rangle = 1$ for the state vector (5) we immediately find the relation

$$\sum_n |\psi_n(t)|^2 = 1 . \tag{6}$$

The state vector (5) evolves according to the time-dependent Schrödinger equation

$$i\hbar(\partial/\partial t)|\Psi(t)\rangle = H|\Psi(t)\rangle , \tag{7}$$

with the Hamiltonian (1) in which the displacements

$\alpha_n(t)$ and $\beta_n(t)$ are classical quantities. Therefore, the total Lagrangian

$$\mathcal{L}=\left\langle\Psi\left|i\hbar\frac{\partial}{\partial t}-H\right|\Psi\right\rangle+\mathcal{L}_{\text{lat}}\ , \tag{8}$$

with

$$\mathcal{L}_{\text{lat}}=\mathcal{L}_{\text{ac}}+\mathcal{L}_{\text{opt}}\ , \tag{9}$$

where

$$\mathcal{L}_{\text{ac}}=M_a\sum_n\left[\frac{1}{2}\dot{\alpha}_n^2-v_0^2U\left[\frac{\alpha_{n+1}-\alpha_n}{l}\right]\right]\ , \tag{10}$$

and

$$\mathcal{L}_{\text{opt}}=M_0\sum_n\left[\frac{1}{2}\dot{\beta}_n^2-l^2\omega_0^2V\left[\frac{\beta_n}{l}\right]\right]\ , \tag{11}$$

can be introduced. Here M_a is the molecule (PG) mass, and M_0 is the reduced mass of the intramolecular atoms (diatomic subsystem). The dimensionless potentials U (intermolecular) and V (intramolecular) are assumed to have single-minimum topology. They are normalized in such a way that their second derivatives at minima are equal to unity, i.e., $U''(0)=1=V''(0)$. The velocity v_0 is the speed of sound in the chain, and the parameter ω_0 describes the frequency of small-amplitude oscillations of the diatomic subsystem. The dot over α_n and β_n denotes the differentiation with respect to time t. Calculating the average

$$\left\langle\Psi\left|i\hbar\frac{\partial}{\partial t}-H\right|\Psi\right\rangle=\sum_n\psi_n^*(i\hbar\dot{\psi}_n-E_n\psi_n+J_{n-1}\psi_{n-1}+J_n\psi_{n+1})\ , \tag{12}$$

we find from the "least action principle,"

$$\delta\int_{t_1}^{t_2}\mathcal{L}(\dot{\psi}_n,\psi_n,\dot{\alpha}_n,\alpha_n,\dot{\beta}_n,\beta_n)dt=0\ , \tag{13}$$

the following set of three difference-differential equations:

$$i\hbar\dot{\psi}_n=E_n\psi_n-(J_{n-1}\psi_{n-1}+J_n\psi_{n+1})\ , \tag{14}$$

$$\begin{aligned}M_a\ddot{\alpha}_n=M_a\frac{v_0^2}{l}&\left[U'\left[\frac{\alpha_{n+1}-\alpha_n}{l}\right]-U'\left[\frac{\alpha_n-\alpha_{n-1}}{l}\right]\right]\\&+\chi_L(|\psi_{n+1}|^2-|\psi_n|^2)+\chi_R(|\psi_n|^2-|\psi_{n-1}|^2)\\&+2\chi_J\,\mathrm{Re}[\psi_n^*(\psi_{n+1}-\psi_{n-1})]\ ,\end{aligned} \tag{15}$$

$$M_0\ddot{\beta}_n=-lM_0\omega_0^2V'(\beta_n/l)-\chi_H|\psi_n|^2\ . \tag{16}$$

Here the functions E_n and J_n are given by the linear expansions (3) and (4).

The conjugated momenta are defined in the standard manner:

$$\begin{aligned}\Pi_n&=\partial\mathcal{L}/\partial\dot{\psi}_n=i\hbar\psi_n^*\ ,\\P_n^a&=\partial\mathcal{L}/\partial\dot{\alpha}_n=M_a\dot{\alpha}_n\ ,\\P_n^0&=\partial\mathcal{L}/\partial\dot{\beta}_n=M_0\dot{\beta}_n\ .\end{aligned} \tag{17}$$

Then the equations of motion (14)–(16) can also be obtained in the usual way from the Hamiltonian

$$\begin{aligned}\mathcal{H}&=\sum_n(i\hbar\psi_n^*\dot{\psi}_n+M_a\dot{\alpha}_n^2+M_0\dot{\beta}_n^2)-\mathcal{L}\\&=\sum_n\psi_n^*(E_n\psi_n-J_{n-1}\psi_{n-1}-J_n\psi_{n+1})+\mathcal{H}_{\text{ac}}+\mathcal{H}_{\text{opt}}\ ,\end{aligned} \tag{18}$$

where $\mathcal{H}_{\text{ac}}$ and $\mathcal{H}_{\text{opt}}$ correspond to $\mathcal{L}_{\text{ac}}$ and $\mathcal{L}_{\text{opt}}$ as presented in (10) and (11).

Note that the Lagrangian given by (8)–(12), or the Hamiltonian given by (18), are written in asymmetric forms. They can be easily transformed to symmetric forms by using the equality

$$\frac{d}{dt}\sum_n|\psi_n(t)|^2=0\ . \tag{19}$$

As a result, we obtain the following expression for the average (see also Ref. 13):

$$\begin{aligned}\left\langle\Psi\left|\left[i\hbar\frac{\partial}{\partial t}-H\right]\right|\Psi\right\rangle=\sum_n[&\tfrac{1}{2}i\hbar(\psi_n^*\dot{\psi}_n-\dot{\psi}_n^*\psi_n)\\&-E_n\psi_n^*\psi_n\\&+J_n(\psi_n^*\psi_{n+1}+\psi_{n+1}^*\psi_n)]\ .\end{aligned} \tag{20}$$

It follows from (20) that the corresponding conjugated momenta for the coordinates ψ_n and ψ_n^* are $(i\hbar/2)\ \psi_n^*$ and $-(i\hbar/2)\psi_n$, respectively. In a similar way, the Hamiltonian $\mathcal{H}$ can also be written symmetrically.

III. DISCRETE NONLINEAR SCHRÖDINGER MODELS

In this section we consider some particular cases of the general set of equations (14)–(16) when discrete nonlinear Schrödinger (NLS) equations can be established. For simplicity we restrict ourselves only to the symmetric case when $\chi_L=\chi_R\equiv\chi_D$. Next, for the sake of simplicity, only harmonic interaction potentials U and V are considered, i.e., these functions are given by

$$U(u)=\tfrac{1}{2}u^2,\quad V(y)=\tfrac{1}{2}y^2\ . \tag{21}$$

The results can be easily extended to more general cases when anharmonicities are important. Let us also neglect the inertia of the molecules, including the motions of their intramolecular atoms; i.e., the time derivatives on the left-hand sides of Eqs. (15) and (16) are assumed to be zero. In each of the following *three* particular cases: (a) $\chi_H=\chi_J=0$ and $\chi_D\neq0$, (b) $\chi_D=\chi_J=0$ and $\chi_H\neq0$, and (c) $\chi_D=\chi_H=0$ and $\chi_J\neq0$, we are able to get from (14)–(16) discrete NLS equations with particular nonlinear terms (i.e., different versions of discretization of the continuum NLS equation). In fact, a discrete NLS equation can be also obtained in the general case when both the acoustic and optical modes are included. In the following, we investigate the various cases separately.

A. Acoustic mode

For the coupling of an excess quantum quasiparticle with the acoustic mode the equations of motion (14) and (15) take the following form [see also (3)]:

$$i\hbar\dot{\psi}_n = E_0\psi_n - J(\psi_{n-1}+\psi_{n+1}) + \chi_D(\alpha_{n+1}-\alpha_{n-1})\psi_n + \chi_J[(\alpha_n-\alpha_{n-1})\psi_{n-1}+(\alpha_{n+1}-\alpha_n)\psi_{n+1}] , \tag{22}$$

$$\ddot{\alpha}_n = \left[\frac{v_0}{l}\right]^2 (\alpha_{n+1}-2\alpha_n+\alpha_{n-1}) + \left[\frac{\chi_D}{M_a}\right](|\psi_{n+1}|^2-|\psi_{n-1}|^2) + \left[\frac{2\chi_J}{M_a}\right]\mathrm{Re}[\psi_n^*(\psi_{n+1}-\psi_{n-1})] . \tag{23}$$

It is convenient to rewrite these equations in dimensionless forms by introducing the scaled (dimensionless) time

$$\tau = v_0 t/l , \tag{24}$$

as well as the following new functions:

$$\phi_n(\tau) = (\pm 1)^n \exp[(i/\hbar)(E_0-2|J|)t]\psi_n(t) , \tag{25}$$

and

$$u_n(\tau) = \alpha_n(t)/l . \tag{26}$$

Then Eqs. (22) and (23) are transformed into [where, for a moment, we allow U to be more general than (21)]

$$i(d\phi_n/d\tau) = -D(\phi_{n+1}-2\phi_n+\phi_{n-1}) + \tfrac{1}{2}g\{c(u_{n+1}-u_{n-1})\phi_n + (1-c)[(u_n-u_{n-1})\phi_{n-1} + (u_{n+1}-u_n)\phi_{n+1}]\} , \tag{27}$$

$$d^2u_n/d\tau^2 = -(\partial/\partial u_n)[U(u_n-u_{n-1})+U(u_{n+1}-u_n)] + g\sigma\{(c/2)(|\phi_{n+1}|^2-|\phi_{n-1}|^2) + (1-c)\,\mathrm{Re}[\phi_n^*(\phi_{n+1}-\phi_{n-1})]\} . \tag{28}$$

Here, for convenience, the dimensionless parameters

$$D = \frac{l|J|}{\hbar v_0} ,\quad c = \frac{\chi_D}{\chi_D+|\chi_J|} ,\quad g = \frac{2l^2(\chi_D+|\chi_J|)}{\hbar v_0} ,\quad \sigma = \frac{\hbar}{lM_a v_0} , \tag{29}$$

have been introduced. Note that $0 \le c \le 1$ holds.

Neglecting the inertia term on the left-hand side of Eq. (28), i.e., assuming that $d^2u_n/d\tau^2=0$, we obtain the following discrete relation between the deformation of the chain and the wave function:

$$U'(u_{n+1}-u_n) = -\tfrac{1}{2}g\sigma[c(|\phi_n|^2+|\phi_{n+1}|^2) + (1-c)(\phi_n^*\phi_{n+1}+\phi_{n+1}^*\phi_n)] . \tag{30}$$

This equation can be solved with respect to $u_{n+1}-u_n$ for quite general functions $U(u_{n+1}-u_n)$. For negative values of $u_{n+1}-u_n$, when the chain is compressed, the function $U(u_{n+1}-u_n)$ and its derivatives are increasing when $u_{n+1}-u_n$ is decreasing. Therefore, for negative values of $u_{n+1}-u_n$, Eq. (30) has a unique solution. This solution may be substituted into Eq. (27) to create a discrete NLS equation. Depending on the function U, a whole family of discrete NLS models may be obtained. In the continuum limit soliton solutions for this general case have been studied in Ref. 20. In the two particular cases, when the function U is quadratic or contains additionally a cubic anharmonicity, the solution for $u_{n+1}-u_n$, and therefore the corresponding discrete NLS equations, can be written explicitly. In the continuum limit the effect of a cubic anharmonicity in the Davydov model has been studied in Ref. 21. Here we restrict ourselves only to the case of a quadratic function U. In this case we obtain the following discrete NLS equation:

$$\begin{aligned} i(d\phi_n/d\tau) = {} & -D(\phi_{n+1}-2\phi_n+\phi_{n-1}) \\ & -(\lambda/4)\{c^2(|\phi_{n-1}|^2+2|\phi_n|^2+|\phi_{n+1}|^2)\phi_n \\ & +c(1-c)[(\phi_{n-1}^*+\phi_{n+1}^*)\phi_n^2+2|\phi_n|^2(\phi_{n-1}+\phi_{n+1})+|\phi_{n-1}|^2\phi_{n-1}+|\phi_{n+1}|^2\phi_{n+1}] \\ & +(1-c)^2[\phi_n^*(\phi_{n-1}^2+\phi_{n+1}^2)+(|\phi_{n-1}|^2+|\phi_{n+1}|^2)\phi_n|\} , \end{aligned} \tag{31}$$

where we have introduced the new coupling constant

$$\lambda = g^2\sigma . \tag{32}$$

In the two limiting cases $c=0$ or $c=1$, Eq. (31) can be essentially simplified. Note that the case $c=1$ corresponds to the original Davydov model.

In the continuum limit ($n \to x$), Eq. (31) admits soliton solutions. For simplicity of notations, in the following we consider only the two special cases with $c=1$ and $c=0$, respectively.

Substituting the expression

$$\phi_n(\tau)=\varphi_n \exp[i(nk-\mathcal{E}\tau)] , \tag{33}$$

with the real functions $\varphi_n(\tau)$ and the (dimensionless) energy $\mathcal{E}$ (to be determined), into Eq. (31) we find for $c=1$ the two equations

$$d\varphi_n/d\tau=D \sin k(\varphi_{n-1}-\varphi_{n+1}) , \tag{34}$$

and

$$\begin{aligned}-D \cos k(\varphi_{n+1}-2\varphi_n+\varphi_{n-1})&\\ -(\lambda/4)(\varphi_{n-1}^2+2\varphi_n^2+\varphi_{n+1}^2)\varphi_n&\\ =[\mathcal{E}-4D \sin^2(k/2)]\varphi_n , &\end{aligned} \tag{35}$$

which, in the continuum limit, are transformed into

$$\varphi_\tau=-2D \sin k\varphi_x , \tag{36}$$

and

$$-D \cos k\varphi_{xx}-\lambda\varphi^3=\varepsilon\varphi . \tag{37}$$

The energy shift is $\varepsilon=\mathcal{E}-4D \sin^2(k/2)$. For waves with a stationary profile ($\xi=x-s\tau$) Eq. (36) gives the relation

$$s=2D \sin k , \tag{38}$$

between the (group) velocity s and the wave number k. On the other, Eq. (37) admits the well-known bell-shaped solution,

$$\varphi(\xi)=(\mu/2)^{1/2}\text{sech}(\mu\xi) , \tag{39}$$

for the envelope, normalized by the condition (6). In the continuum limit the latter can be rewritten as

$$\int \varphi^2(\xi)d\xi=1 . \tag{40}$$

The inverse half-width μ of the soliton is given by

$$\mu=\mu(k)=\lambda/4D \cos k . \tag{41}$$

The value of the spectral parameter ε [of the nonlinear eigenvalue problem (37)], which corresponds to the soliton level (39), is represented by

$$\varepsilon(k)=-D \cos k\mu^2=-\lambda^2/16D \cos k . \tag{42}$$

Due to the relation (38) the parameters (41) and (42) depend on the soliton velocity s. We have $D \cos k=(1/2)(s_0^2-s^2)^{1/2}$, where $s_0=2D$ is the maximum value of the group velocity s [see (38)] of the propagation of the exciton waves with the linear dispersion law

$$\mathcal{E}(k,\varphi_0)=4D \sin^2(k/2) , \tag{43}$$

which describes the exciton band with the width $4D$. The parameters $\varepsilon(k)$ and $\mu(k)$ can be rewritten as

$$\varepsilon\equiv\varepsilon(s)=-(\lambda^2/8)(s_0^2-s^2)^{-1/2}$$

and (44)

$$\mu\equiv\mu(s)=(\lambda/2)(s_0^2-s^2)^{-1/2} .$$

It follows from these expressions that the spectrum of admissible soliton velocities s is $0\le s<s_0$.

Having the soliton profile for the envelope (39), from the relation (30) the profile for the relative displacement field $r=u_x$ can be immediately found. Using (39) and (44) we obtain

$$r(\xi)=-r_0 \,\text{sech}^2(\mu\xi) , \tag{45}$$

with the amplitude

$$r_0=(\lambda^{3/2}/4)(s_0^2-s^2)^{-1/2} . \tag{46}$$

Now we compare the soliton solution given by (39) and (44)–(46) with the *exact* soliton solution when the inertia term in Eq. (28) is kept. Again, we still consider the simplest case with $c=1$. Substituting the ansatz (33) into Eqs. (27) and (28) (for $c=1$ in the continuum limit) we arrive at (36) and the equations

$$-D \cos k\varphi_{xx}+gr\varphi=\varepsilon\varphi , \tag{47}$$

$$r_{\tau\tau}-r_{xx}=g(\varphi^2)_{xx} . \tag{48}$$

The soliton solutions of these equations are well known and are given by the same formulas (39) and (45). However, the parameters ε, μ, and r_0 now contain the additional factor $(1-s^2)^{-1}$, i.e., [cf. (44) and (46)],

$$\begin{aligned}\varepsilon&=-(\lambda^2/8)(s_0^2-s^2)^{-1/2}(1-s^2)^{-2} ,\\ \mu&=(\lambda/2)(s_0^2-s^2)^{-1/2}(1-s^2)^{-1} ,\\ r_0&=(\lambda^{3/2}/4)(s_0^2-s^2)^{-1/2}(1-s^2)^{-2} .\end{aligned} \tag{49}$$

Therefore, the soliton velocity spectrum is reduced if $s_0>1$. But as well shall see below, realistic parameter values lead to $s_0<1$. It can be seen from (49) that the influence of the factor $(1-s^2)^{-1}$ is not so large if $s_0<1$, especially for small velocities s. Thus, the stronger condition $s_0\ll 1$ (as used, for example, in Ref. 22) for the neglect of the inertia of the chain molecules is not so important; it is sufficient to assume $s_0<1$. In fact, we cannot be close to the characteristic velocity s_0, since in this case the inequality $r_0>1$ will hold. From the physical point of view this inequality is forbidden because neighboring molecules cannot pass through each other when the soliton compression of the chain appears. Therefore, the inequality $r_0<1$ must be always fulfilled and the velocity spectrum $0\le s<s_0$ will be more shortened.

Now we consider the other case, when $c=0$. In the same way as before, from Eq. (31) (with $c=0$) we find

$$\begin{aligned}d\varphi_n/d\tau=\sin k(\varphi_{n-1}-\varphi_{n+1})&\\ \times[D+(\lambda/2)\cos k\varphi_n(\varphi_{n-1}+\varphi_{n+1})] ,&\end{aligned} \tag{50}$$

$$\begin{aligned}-D \cos k(\varphi_{n+1}-2\varphi_n+\varphi_{n-1})&\\ -(\lambda/2)\cos^2 k(\varphi_{n-1}^2+\varphi_{n+1}^2)\varphi_n=\varepsilon\varphi_n .&\end{aligned} \tag{51}$$

Eq. (50) is much more complicated than the previous equation (34) because of the additional term in the square brackets. However, due to the normalization condition (40), for broad solitons, spreading over many sites of the chain, the inequality $\varphi_n\ll 1$ must be satisfied. Therefore, if the coupling constant λ is not large the second term in the square brackets of Eq. (50) may be dropped and therefore the relation (38) between s and k may be considered still valid, probably slightly modified due to this nonlinear term. In the continuum limit the other equation (51) is transformed into

$$-D\cos k\varphi_{xx}-\lambda\cos^2 k\varphi^3=\varepsilon\varphi\ . \tag{52}$$

This equation has the same form as Eq. (37) and therefore admits the same soliton solution given by (39), (41), (42), and (44)–(46), where instead of λ the parameter $\lambda\cos^2 k$ should be substituted. In the general case $0\le c\le 1$ more nonlinear terms of the same type appear in Eq. (50). Using the same arguments as before we adopt the relation (38) also in the general case. The second equation contains many nonlinear terms (we do not write them here), but in the continuum limit the form which generalizes Eqs. (37) and (52) is

$$-D\cos k\varphi_{xx}-\lambda[c+(1-c)\cos k]^2\varphi^3=\varepsilon\varphi\ . \tag{53}$$

Therefore, again all the previous formulas for the Davydov soliton may be used, but the coupling λ should be replaced by $\lambda[c+(1-c)\cos k]^2$. With the same substitution ($\lambda\rightarrow\lambda[c+(1-c)\cos k]^2$) in (42) the nonlinear dispersion law is also obtained in the general case.

B. Optical mode

In the case of the coupling of an excess quantum quasiparticle with only the optical mode (in a diatomic subsystem) the basic equations of motion (14) and (16) describe the well-known Holstein model. From these equations, with the assumptions $\chi_L=\chi_R=\chi_J=0$ and $\alpha_n\equiv 0$, we obtain [see also (3)]

$$i\hbar\dot{\psi}_n=E_0\psi_n-J(\psi_{n-1}+\psi_{n+1})+\chi_H\beta_n\psi_n\ , \tag{54}$$

and

$$\ddot{\beta}_n=-\omega_0^2\beta_n-(\chi_H/M_0)|\psi_n|^2\ . \tag{55}$$

Similarly, using the dimensionless time

$$\tau=\omega_0 t\ , \tag{56}$$

the functions (25), and

$$y_n(\tau)=\beta_n(t)/l\ , \tag{57}$$

[cf. (24) and (26)], we obtain the dimensionless equations

$$i(d\phi_n/d\tau)=-D(\phi_{n+1}-2\phi_n+\phi_{n-1})+gy_n\phi_n\ , \tag{58}$$

and

$$\frac{d^2y_n}{d\tau^2}=-y_n-g\sigma|\phi_n|^2\ . \tag{59}$$

The parameters D, g, and σ are given now by [cf. (29)]

$$D=\frac{|J|}{\hbar\omega_0},\quad g=\frac{l\chi_H}{\hbar\omega_0},\quad \sigma=\frac{\hbar}{l^2M_0\omega_0}\ . \tag{60}$$

Contrary to the case of the Davydov solitons, we are not able to solve the continuum limit of Eqs. (58) and (59) exactly in the presence of the inertia term on the left-hand side of Eq. (59). On the other hand, the coupled equations (58) and (59) can be solved by using an appropriate set of trial functions, and their dynamical stability is easily established by using numerical techniques.[23] For sufficiently small soliton velocities we write

$$y_n=-g\sigma|\phi_n|^2\ , \tag{61}$$

and arrive at the following NLS equation in the most simple discretization:

$$i(d\phi_n/d\tau)=-D(\phi_{n+1}-2\phi_n+\phi_{n-1})-\lambda|\phi_n|^2\phi_n\ , \tag{62}$$

where the nonlinearity parameter λ is given by the relation (32). Similarly to the Davydov model, the intramolecular potential $V(y_n)$ may be considered to be of a general form.[23] In this case the nonlinear term in Eq. (62) will be generalized to $\lambda f(|\phi_n|^2)\phi_n$ with some monotonically increasing function f.

Substituting (33) into Eq. (62), in the continuum limit we get Eqs. (36) and (37), whose soliton solutions have been already analyzed and are given by (39) and (44)–(46). But the parameters for this solution are given now by (60) [see also (32)].

Thus, we have illustrated in this section that the problem of the interaction of an excess quantum quasiparticle (an excess electron in the conduction band or a quantum of the intramolecular exciton amide-*I*) can be reduced to discrete NLS equations. The discrete forms of the nonlinear terms in these equations depend on the types of the displacement fields with which the quasiparticle interacts. The resulting discrete NLS equations cannot be solved analytically, but in the continuum limit they are transformed to the well-known integrable cubic NLS equation. It should be also emphasized here that the case of the discrete NLS equation with the Ablowitz-Ladik discretization[24] cannot be reached in this (acoustic or optical polaron) problem.

IV. PARAMETER VALUES

In this section we discuss the parameter values which should be chosen when the theory is applied to realistic situations. We also need to know, for which parameter ranges the soliton solutions presented in Sec. III are valid, in which cases the states are strongly localized, etc.

As was mentioned in Sec. I, the quantum energy of an amide-*I* vibration is $E_0=1665\ \text{cm}^{-1}\hat{=}0.206$ eV. As for the lattice spacing l of the molecular chain, one should notice that the three-dimensional structure of protein is rather complex, but one can identify certain substructures within it. There are helical arrangements and planar structures. One of the most common helical structures is the α helix. For the reason of simplicity, we restrict ourselves in this paper only to the simplest one-chain model; a more realistic model of the α helix consists of three coupled regular chains. As previously,[8–13] we take for the lattice spacing of the molecular chain the value $l=4.5$ Å which can be also adopted to the one-chain model of ACN crystals.[17] The mass of a PG is usually taken (see, for instance Ref. 8) to be $\tilde{M}_a = 114.2 m_p = 1.91 \times 10^{-25}$ kg, where $m_p = 1.6726 \times 10^{-27}$ kg is the proton mass. If we consider only the symmetric mode of the α-helix vibration (i.e., ϕ_n is the same for different chains of the helix) the effective mass is $M_a = 3\tilde{M}$.[13] For the reduced mass of intramolecular low-frequency optical vibrations we may choose the value $M_0 = m_p$.

As in Refs. 8 and 9, for both the acoustic and optical mode we use the value $\tilde{K}_a = K_0 = 13 N/m$ for the stretching force constant of the hydrogen bond which has been determined experimentally by Itoh and Shimanouchi[25] from the vibrational spectra of crystalline formanide. For the same reason as above, the effective force for the α helix is $K_a = 3\tilde{K}_a$ (see also Ref. 13). Then the velocity of longitudinal sound in the chain is $v_0 = (K_a/M_a)^{1/2} l = 3.715 \times 10^3$ m/s. The characteristic frequency of the low-frequency optical oscillations is given by the value $\omega_0 = (K_0/M_0)^{1/2} = 88.16 \times 10^{12}$ s^{-1} ($\hbar\omega_0 = 46.9$ cm^{-1}).

The hopping term in the Hamiltonian (1) with the coefficients J_n represents the dipole-dipole coupling of an amide-*I* quantum at any molecule of the chain to its neighbors. The values for these coupling coefficients [in our notations J, see (4)] have been calculated by Nevskaya and Chirgadze.[26] Therefore, the value $J = 7.8$ cm^{-1} $= 1.55 \times 10^{-22}$ J has been chosen for the α helix[8] and the value $J = 4$ cm^{-1} is usually taken for an ACN molecule.[17]

Finally, the nonlinear coupling coefficients χ_D, χ_J, and χ_H are allowed to be adjustable parameters.[8,17] With their help we are able to control the soliton width, to create strongly self-trapped states which appear to be immobile, etc. Some rough estimates for the coefficient χ_D are outlined in Ref. 8. They indicate that $\chi_D \sim 2{-}6 \times 10^{-11} N$. The coefficient χ_J is usually smaller than χ_D, so it may be taken as $\chi_D \sim 10^{-11} N$. Next, the value for the parameter χ_H has been approximately estimated in Ref. 17, and it is proved to be $\chi_H = 6.2 \times 10^{-11} N$. This value leads to the existence of stationary, strongly localized states. In order to allow mobile soliton states to exist some smaller values for χ_H should be also considered. The value $\chi_H = 2.5 \times 10^{-11} N$ appears to be appropriate for the existence of mobile solitons.[27]

Now, all the parameter values considered above may be transformed to the corresponding dimensionless values according to the relations (29), (32), and (60). All these dimensionless values are summarized in Tables I, II, and III. The generally accepted fixed parameter values are listed in Table I. Here, we also present the time units (t.u.), l/v_0 for the acoustic model [see (24)], and ω_0^{-1} for the optical model [see (56)], as well as the dimensionless values for the amide-*I* quantum energy E_0, which appear in our dimensionless description to be different: $\epsilon_0 = lE_0/\hbar v_0$ and $\epsilon_0 = E_0/\hbar\omega_0$, respectively. In Tables II and III we have listed the dimensionless nonlinear coupling constants g and λ [see (32)] for both the models as well as the corresponding values for the half inverse width of the sech-soliton solution at rest. This quantity μ_0 is given by (41) with $k=0$ ($s=0$). We should also check the inequality $r_0 < 1$ (discussed in Sec. III) for the amplitude of the relative displacement field in Davydov's soliton. For very narrow solitons with $\mu_0 = 1.25$ ($\chi_D = 5 \times 10^{-11} N$) the amplitude r_0 does not exceed 0.6. This amplitude decreases with enlarging the soliton width and therefore the condition $r_0 < 1$ is fulfilled. The analytical soliton solution (39) is valid if $\mu \ll 1$. It can be seen from Tables II and III that this solution can be used for sufficiently small values of the coupling constants χ_D or χ_H ($\chi_D \sim 1{-}2 \times 10^{-11} N$ and $\chi_H \sim 1 - 3 \times 10^{-11} N$). Also note that the maximum group velocity of exciton waves ($s_0 = 2D = 0.356$) is smaller than the speed of longitudinal sound in the chain.

TABLE I. Fixed parameter values for the acoustic (Davydov) and optical (Holstein) models.

Dimensionless quantities	Davydov model, see Eq. (29)	Holstein model, see Eq. (60)
t.u. (10^{-14} s)	$l/v_0 = 12.10$	$\omega_0^{-1} = 1.13$
ϵ_0	37.94	3.55
D	17.8×10^{-2}	8.5×10^{-3}
σ	1.1×10^{-4}	35.4×10^{-4}

V. ONE-QUANTUM DYNAMICS IN A RANDOM MOLECULAR CHAIN

Here we study the discrete time-dependent NLS models presented by Eqs. (31) and (62). As usual (see, for example, Refs. 19, 29, and 30), a random potential V_n can be introduced on the right-hand sides of these equations. From the physical point of view in the case of biological molecules the origin of this potential can be motivated as follows: Usually, any biomolecular chain can be found in a random environment consisting of some molecules randomly distributed around this chain (see empty circles in Fig. 1). The interaction of the chain molecules with molecules of the environment naturally leads to some shift of the energy levels E_n which can be explained exactly in the same way as the appearance of the energy shift [see (3)] caused by the dynamical variables α_n and β_n. Therefore, the constant energy $E_0 = 1665$ cm^{-1} in the expansion (3) may be substituted by a random field $E_{0,n}$ centered around the value E_0. This can be taken care of by the random potential V_n.

TABLE II. Adjustable parameter values for the Davydov model ($\chi_J = 0$).

$\chi_D (10^{-11} N)$	g	λ	μ_0
1	10.32	0.04	0.05
2	20.65	0.14	0.20
3	30.97	0.32	0.45
4	41.29	0.57	0.80
5	86.03	0.89	1.25

The second natural randomness in biological molecules

TABLE III. Adjustable parameter values for the Holstein model.

$\chi_H(10^{-11}N)$	g	$\lambda(10^{-3})$	μ_0
1	0.48	0.8	0.02
2	0.97	3.3	0.10
3	1.45	7.4	0.22
4	1.93	13.2	0.39
5	2.42	20.7	0.61
6	2.90	29.8	0.87
6.2	3.00	31.8	0.93
7	3.38	40.5	1.19

has to appear owing to the different masses of PG's including their side groups. Therefore, the mass M_a in the equations of motion for a realistic chain should be substituted by M_n [31] and therefore the dimensionless parameter σ in (32) should be replaced by σ_n [see (29)]. The reduced mass M_0 and/or the frequency ω_0 can be also distorted randomly by the environment. Thus, in Eqs. (31) and (62) we may substitute the nonlinear coupling constant λ by λ_n.

Finally, the third type of randomness which should be included into the discrete NLS models originates from a possible random distribution of the intermolecular distances or orientations of neighboring PG's [31]. A random distribution of the intersite coupling constants may occur in addition to the constant J in (4). Therefore, in Eqs. (31) and (62) a random field D_n should be incorporated. Thus, for instance in the case of the Holstein model, one can write

$$i(d\phi_n/d\tau)+D_n(\phi_{n+1}-\phi_n)-D_{n-1}(\phi_n-\phi_{n-1}) +\lambda_n|\phi_n|^2\phi_n=V_n\phi_n \ . \tag{63}$$

We come back to this equation, and similar models for random molecular chains, in the next section. Before presenting numerical simulations, some analytical estimates are appropriate.

The nonlinear wave propagation described by Eq. (63) can be modeled by a corresponding dynamical equation for a particle moving in an effective force field. To establish such an equation, we consider the probability density $|\psi_n|^2$ (or $|\phi_n|^2$) in the normalization condition (6) as the mass density of an effective spatially extended particle. Then the relation

$$\sum_n |\phi_n(\tau)|^2=1 \tag{64}$$

means that the total mass of the particle is unity. Next, we introduce the following two averaged quantities:

$$X(\tau)=\sum_n n|\phi_n|^2 \ , \tag{65}$$

i.e., the particle position, and

$$s(\tau)=i\sum_n D_n[(\phi^*_{n+1}-\phi^*_n)\phi_n-\phi^*_n(\phi_{n+1}-\phi_n)] =i\sum_n D_n(\phi^*_{n+1}\phi_n-\phi^*_n\phi_{n+1}) \ , \tag{66}$$

the particle velocity. Note that in the continuum limit the last relation transforms to (38). That is why we use the same notation s. Using Eq. (63), it can be shown that

$$dX/d\tau=s \quad \text{and} \quad ds/d\tau=F \ , \tag{67}$$

where the effective force F is given by

$$F(\tau)=\sum_n \{D_n[(D_{n-1}-D_{n+1}) +(\lambda_{n+1}|\phi_{n+1}|^2-\lambda_n|\phi_n|^2) +(V_n-V_{n+1})](\phi^*_{n+1}\phi_n+\phi^*_n\phi_{n+1})\} \ . \tag{68}$$

Each of the three terms in the square bracket of (68) represents local forces in the chain, and that is why they are represented by differences. The total force F is obviously the weighted sum, but the measure is $\frac{1}{2}(\phi^*_{n+1}\phi_n+\phi^*_n\phi_{n+1})$ instead of $|\phi_n|^2$. This difference is caused by the degree of intersite coupling in the chain. For example, in the case of strongly localized states, when the excitation is mainly located at one site (molecule), the measure $\frac{1}{2}(\phi^*_{n+1}\phi_n+\phi^*_n\phi_{n+1})$ tends to zero everywhere in the chain, and therefore the effective force (68) disappears. Indeed, if the excitation is trapped locally by some site, there is no force to move it from there. It is important to note that this is a discreteness effect, and in the continuum limit this measure is transformed to $|\phi(x,\tau)|^2$. Therefore, in the discrete case the force (68) contains more information than in its continuum limit. In the latter case $D_n\to D(x)$, $\lambda_n\to\lambda(x)$, $V_n\to V(x)$, and the expression (68) takes the form

$$F=-2\int D\left[\frac{\partial}{\partial x}(2D-\lambda|\phi|^2+V)\right]|\phi|^2dx \ . \tag{69}$$

In the particular case, when the randomness in the chain is given only by the function $V(x)$, i.e., $D(x)=\text{const}$ and $\lambda(x)=\text{const}$, the expression (69) is reduced to the corresponding formula in Ref. 19 [note that $\phi(\pm\infty,\tau)=0$]. In a similar way, we can represent the motion of a single particle under the force (69) in an equivalent potential. Let us introduce new functions $W_1(x)$ and $W_2(x)$ according to the equations

$$W_1'=D\lambda' \quad \text{and} \quad W_2'=DV' \ , \tag{70}$$

where the prime denotes the differentiation with respect to x. Assuming the field intensity $|\phi|^2$ to be a function of τ only through $x-X(\tau)$, after integration of (69) by parts we find that $F[X(\tau)]=-\partial W(X)/\partial X$, with the effective potential

$$W(X)=2\int[(\tfrac{1}{2}D\lambda-W_1)|\phi|^2+D^2+W_2]|\phi|^2dx \ . \tag{71}$$

This expression may be considered as a generalization of the corresponding formula of Ref. 19 when other types of randomness are included into the model.

VI. NUMERICAL SIMULATIONS

The model equations derived in the previous sections form the basis for evaluating transport of vibrational energy in molecular chains. Here we report on some simulations (a complete scenario of the various effects will be presented in a subsequent paper) which demonstrate the importance of nonlinearities, and in particular soliton solutions, for the transport. Without randomness, it is well known that modulational instability can lead in the continuous NLS equation to soliton solutions. The modulational instability in discrete molecular chains is discussed in Appendix A. There are many interesting phenomena due to discreteness (especially when the solutions become narrow). Important for the present investigation is that for Eq. (31) (e.g., for $c=1$) and Eq. (62) modulational instability and subsequent soliton formation can take place in the region of parameter values under consideration. In addition, randomness will not forbid soliton formation. We do not want to discuss all the numerical details associated with soliton generation in random media since the main emphasis is on the models and their validities in random molecular chains. But we want to supplement the analytical models by some numerical simulations which show the new effect caused by solitons. As a paradigm for nonlinear effects in a random molecular chain we take the equation

$$i(d\varphi_n/d\tau)+(\varphi_{n+1}-2\varphi_n+\varphi)_{n-1}+\lambda|\varphi_n|^2\varphi_n=V_n\varphi_n\ , \tag{72}$$

which corresponds to the Holstein model in random potential V_n.

When propagation of vibrational energy in a *linear* random molecular chain is investigated, localization can occur which leads to an exponential decay of the transmission coefficient. Following the pioneering work of Anderson[18] there exists a huge literature, including numerical work, on the localization. We show in Fig. 2 a typical result of Anderson localization in a *linear* random molecular chain for two reasons. First, we want to demonstrate that our numerical code is able to produce all the interesting aspects. We have tested with various lengths of the chain and different discretizations. All these tests are in agreement with the literature; they also enable us to demonstrate Anderson localization in finite, discrete, and *linear* random molecular chains. Second and most important in the present context, we have reference states for comparison with results for *nonlinear* random molecular chains.

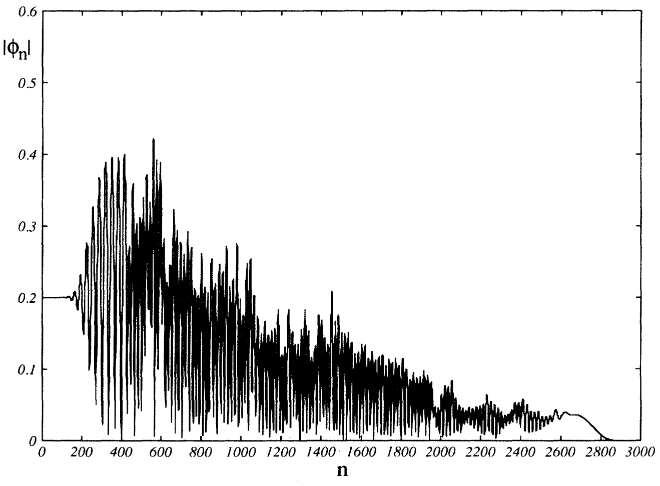

FIG. 2. Decay of vibrational excitation in a linear random molecular chain. Equation (63) is solved for $D_n=D_{n-1}=1$ and $\lambda_n\equiv 0$. V_n is a random potential with the mean value -9 and a mean standard derivation of 8. The chain is driven by an oscillation (with frequency $\omega=4$) at $n=0$. Note that the first and last 400 points simulate open ends with strong damping of the reflected and transmitted waves, respectively.

Let us explain a little bit more in detail how the numerical code works. A "plane wave" is penetrating from the left into a random potential. By "plane wave" we mean the boundary condition of a prescribed oscillation at $n=0$. In the results shown in Fig. 2, the oscillation is transformed out and, because of numerical reasons, the chain is extended further to the left (first 400 points) to establish an adiabatic onset of the oscillations and to suppress reflections from the left. On the average (with different realizations of the random potential), an exponential decay can be found. Again, beyond the *finite* random molecular chain, we also have at the right side some extension of the chain (last 400 points) in order to avoid reflections from the right. (Details and more results will be published in a forthcoming paper.)

Now the interesting point: We have allowed nonlinear contributions besides the random potential. The simulations shown in Fig. 3 are for Eq. (72) [Eq. (63) when $D_n=D=\text{const}$, $\lambda_n=\lambda=\text{const}$, but V_n random]. The initial energy of the excitation is such that classical motion above the potential maxima is not forbidden. In the linear case we know that due to phase interferences an exponential decay can occur. [Note that in Fig. 3(a) we have used the same boundary conditions as in Fig. 2.] However, because of nonlinearity, solitons can be formed; they can easily override the potential fluctuations and contribute to an enhanced transport. This is demonstrated also in Fig. 3(b), where a special section of the chain is shown, and a peak is identified as a soliton. When the sign of λ is reversed, this effect disappears. When we analyze the results shown in Fig. 3(a), especially with a greater spatial resolution [see Fig. 3(b)], we clearly can identify the several peaks as soliton solutions. From here we conclude that in a nonlinear random molecular chain transport of vibrational energy can take place via solitons. That means that the transmission coefficient will not decay exponentially (with length of the chain) as predicted by linear theory. Note that this is an important new effect. Although expected from the theory of nonrandom chains, it adds a very interesting aspect to the importance of solitons in molecular chains. In nonrandom chains solitons are important for stable pulse propagation, overcoming the dispersive spreading of linear wave packets. But in nonrandom chains they do not affect the net transmission coefficient. In random molecular chains, solitons are responsible for stable pulse propagation *and* an enhancement of the transmission coefficient, compared to the linear case.

There are many more interesting results which evolve from our detailed numerics. We cannot present them all here. They will be shown in a subsequent paper. Here, let us only mention one additional point. Besides enhancement of transport, also a reduction can occur when pinned (nonlinear) solutions appear. The latter occur due to discreteness and more attention should be given to them.

VII. SUMMARY AND OUTLOOK

In this paper we have investigated the transport of vibrational energy in a random molecular chain. A generalized model is proposed which does not assume a rigid sublattice. On the contrary, a soft sublattice is allowed, and both the optical and the acoustic modes of the lattice are included. The description reduces in simplified situations to the Davydov model and the Holstein model, respectively. We have further discussed the randomness caused by different physical mechanisms: (i) randomly distributed molecules around the chain, (ii) different masses of the side groups, and (iii) random distributions of the inter-molecular distances. In order to demonstrate a new physical effect, we have simplified further by reducing to discrete nonlinear Schrödinger equations, with random potentials as caused by randomly distributed molecules around the chain. Besides Anderson localization in the (nearly) linear regime, this leads to an anomalous nonlinear convective transport of vibrational energy.

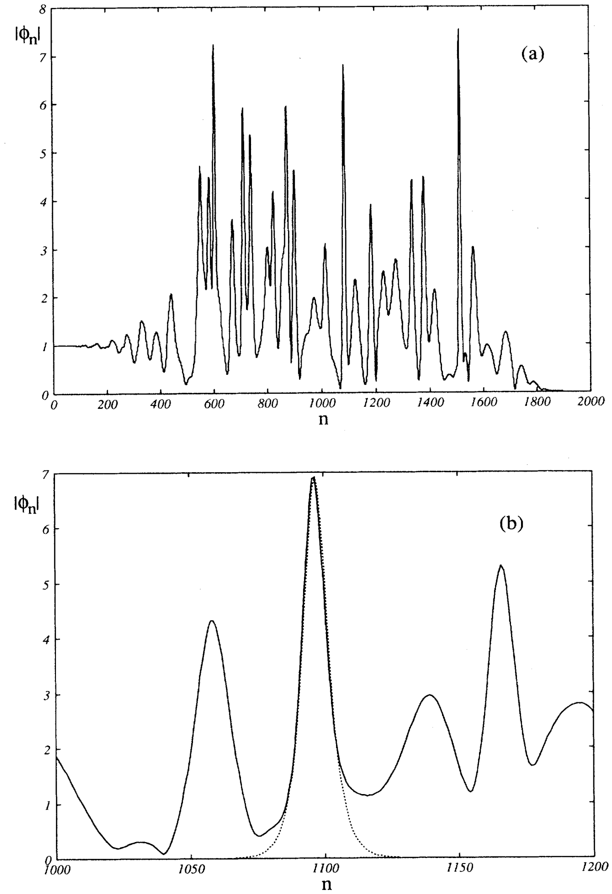

FIG. 3. (a) Transport of vibrational excitation in a nonlinear random molecular chain. Again Eq. (63) is solved for $D_n = D_{n-1} = 1$, but $\lambda_n = \lambda = 1$. The other parameters are $\omega = 1$ for the frequency of the driven molecule at $n = 0$, mean value 0, and mean standard derivation 0.25 for the random potential. Again the first and last 400 points are used to suppress reflections from both ends. (b) Same as Fig. 3(a). Only a section of the chain is shown. The peak appearing around $n = 1500$ is identified as a soliton. The solid line depicts the numerical simulation, whereas the dotted line represents a fit by the analytical soliton formula.

The presentation of numerical results is not complete. Here we have shown a general effect of nonlinearity in discrete random systems. We did not discuss in detail the effects of the different forms of discretization which should be expected because of the different predictions by modulational instability. Also, the influence of very narrow (strongly localized) collective excitations on the nonlinear transport is not worked out here in detail. This will be done in a forthcoming publication where special attention is given to the so-called pinned solitons.

ACKNOWLEDGMENTS

The authors gratefully acknowledge interesting discussions with Dr. Yuri Kivshar. This research was performed under the auspices of the Sonderforschungsbereich 237. It was also supported by the European Community under Contract No. SC1-CT91-0705 and the Ministerium für Wissenschaft und Forschung of North Rhine Westphalia.

APPENDIX A: MODULATIONAL INSTABILITY IN DISCRETE SYSTEMS

In this appendix we discuss the process of generation of solitons in a molecular chain. The effects of discreteness are especially emphasized; randomness is absent.

In the continuum limit, the modulational instability of plane waves is well known. When inserting into

$$i\dot{\varphi} + b\varphi_{xx} + |\varphi|^2\varphi = 0 \tag{A1}$$

a solution

$$\varphi_s(x,t) = e^{i(kx-\omega t)} \text{ with } \omega = bk^2 - 1 , \tag{A2}$$

and subsequently perturbing it in the form

$$\varphi = [1 + a(x,t)]e^{i(kx-\omega t)+ip(x,t)} , \tag{A3}$$

we find linearized equations for the amplitude a and the phase p. Making the ansatz

$$(a,p) = (a_0,p_0)e^{i(Qx-\Omega t)} , \tag{A4}$$

unstable solutions are possible for $b > 0$ and

$$Q^2 < 2/b . \tag{A5}$$

The maximum growth rate $\gamma_{\max} = 1$ follows from the imaginary part of Ω,

$$\gamma = \sqrt{bQ^2(2 - bQ^2)} , \tag{A6}$$

at $Q^2_{\max} = 1/b$. Here we compare these results with those of the three discrete model equations

$$i\dot{\varphi}_n+b(\varphi_{n+1}-2\varphi_n+\varphi_{n-1})+|\varphi_n|^2\varphi_n=0\ , \tag{A7}$$

$$i\dot{\varphi}_n+b(\varphi_{n+1}-2\varphi_n+\varphi_{n-1}) +\tfrac{1}{4}(|\varphi_{n+1}|^2+2|\varphi_n|^2+|\varphi_{n-1}|^2)\varphi_n=0\ , \tag{A8}$$

$$i\dot{\varphi}_n+b(\varphi_{n+1}-2\varphi_n+\varphi_{n-1}) +\tfrac{1}{2}|\varphi_n|^2(\varphi_{n+1}+\varphi_{n-1})=0\ ; \tag{A9}$$

the first two of them arose within the context of molecular chain [Eq. (62) and Eq. (31) for $c=1$, respectively] whereas the last one (Ablowitz-Ladik equation) is included here for the reason of completeness. For (A7) and (A8) we have the nonlinear dispersion relation

$$\omega=4b\sin^2(k/2)-1\ , \tag{A10}$$

and for (A9) we have

$$\omega=4b\sin^2(k/2)-\cos k\ , \tag{A11}$$

instead of (A2). Here, $k\in(-\pi,\pi]$. A similar ansatz as in (A3) and (A4) leads to three different dispersion relations

$$(\Omega-2b\sin Q\sin k)^2=4b\sin^2(Q/2)\cos k[4b\sin^2(Q/2)\cos k-2]\ , \tag{A12}$$

$$(\Omega-2b\sin Q\sin k)^2=4b\sin^2(Q/2)\cos k[4b\sin^2(Q/2)\cos k-2\cos^2(Q/2)]\ , \tag{A13}$$

$$[\Omega-2b\sin Q\sin k(b+\tfrac{1}{2})]^2=4\sin^2(Q/2)\cos^2 k(b+\tfrac{1}{2})[4b\sin^2(Q/2)-2\cos^2(Q/2)] \tag{A14}$$

for (A7)–(A9), respectively. From Eqs. (A12)–(A14) the conditions $b>0$ and

$$\sin^2\left[\frac{Q}{2}\right]<\frac{1}{2b\cos k}\quad\text{and}\quad \cos k>0\ , \tag{A15}$$

$$\sin^2\left[\frac{Q}{2}\right]<\frac{1}{1+2b\cos k}\quad\text{and}\quad \cos k>0\ , \tag{A16}$$

$$\sin^2\left[\frac{Q}{2}\right]<\frac{1}{1+2b} \tag{A17}$$

follow for instability, respectively. They show that discreteness has significant effects on the existence of modulational instability. In the unstable regions, the corresponding growth rates can be obtained from Eqs. (A12)–(A14). Typical results are shown in Fig. 4 for $b=1$ and $k=0.01$.

We have also tested our numerical code by performing numerical simulations. Starting with plane-wave solutions we disturbed these solutions by waves with a certain wave number Q. The growth rates of the perturbations were measured. Typical results are shown in Fig. 4 by marked points. The agreement with the theoretical predictions is excellent. This shows that modulational instability is effective in random molecular chains and that we can trust our numerical code.

APPENDIX B: MULTIPARTICLE GENERALIZATION

So far we have considered the molecular chain in the presence of *one* quantum of the amide-*I* excitation. In this appendix we present a NLS equation for the case when Q quanta (or Q excess noninteracting electrons[32]) can be found in the system. In this case the wave function appears to be Q-dimensional in space.[27,33]

To describe the quantum evolution of an arbitrary conserved number Q of amide-*I* excitation quanta, one can use the generalized Davydov ansatz[27,33]

$$|\Psi_Q(t)\rangle=(Q!)^{-1/2}\sum_{n_1,\ldots,n_Q}\psi_{n_1,\ldots,n_Q}(t)B^\dagger_{n_1}\ldots B^\dagger_{n_Q}|0\rangle\ , \tag{B1}$$

where the probability amplitude $\psi_{n_1,\ldots,n_Q}(t)$ is supposed to be symmetric with respect to any permutation of $n_1,\ldots,n_Q$. It is normalized as

$$\langle\Psi_Q(t)|\Psi_Q(t)\rangle=\sum_{n_1,\ldots,n_Q}|\psi_{n_1,\ldots,n_Q}(t)|^2=1\ , \tag{B2}$$

so that for all times there are Q quanta in the state (B1), i.e.,

$$\langle\Psi_Q(t)|\sum_n B^\dagger_n B_n|\Psi_Q(t)\rangle=Q\ . \tag{B3}$$

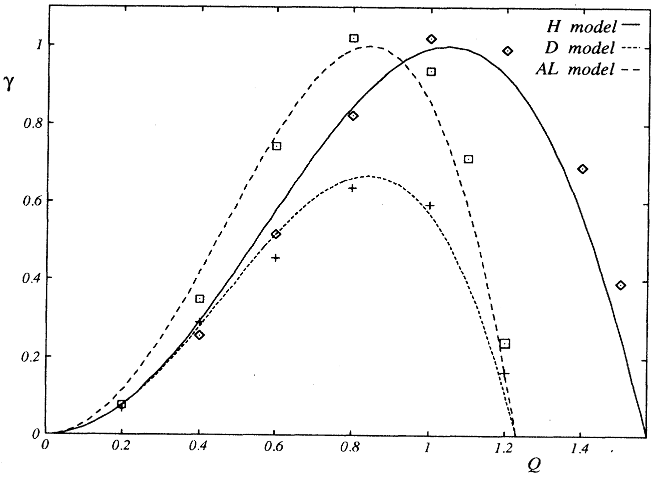

FIG. 4. Growth rates γ vs modulational wave number Q for the three models Eq. (A7), solid line; (A8), broken line; and (A9), dotted line, respectively. The parameter values $b=1$ and $k=0.01$ are chosen. For each model, numerical simulations have been performed which are shown as marked points (◇, +, □, respectively).

Equations of motion for Q quanta, interacting with the acoustic and/or optical mode, which generalize Eqs. (14)–(16) can be derived in the same way as before by using the Lagrangian (8)–(11). For simplicity of notations we restrict ourselves here only to the case of the coupling with an optical mode. As a result, we obtain the following Euler-Lagrange equations [cf. Eqs. (54) and (55)]:

$$\begin{aligned} i\hbar\dot{\psi}_{n_1,\ldots,n_Q} &= QE_0\psi_{n_1,\ldots,n_Q} \\ &\quad -J\sum_{j=1}^{Q}(\psi_{n_1,\ldots,n_j-1,\ldots,n_Q} \\ &\qquad +\psi_{n_1,\ldots,n_j+1,\ldots,n_Q}) \\ &\qquad +\chi_H\left[\sum_{j=1}^{Q}\beta_{n_j}\right]\psi_{n_1,\ldots,n_Q}\,, \end{aligned} \tag{B4}$$

and

$$\ddot{\beta}_n=-\omega_0^2\beta_n-Q\chi_H\sum_{n_1,\ldots,n_{Q-1}}|\psi_{n_1,\ldots,n_{Q-1}n}|^2\,. \tag{B5}$$

Similar to the particular case $Q=1$ (see Sec. IIIB), these equations can also be written in the dimensionless (canonical) form if we introduce the notations (56) and (57) as well as the new (Q-dimensional) wave function

$$\begin{aligned} \phi_{n_1,\ldots,n_Q}(\tau) &= \prod_{j=1}^{Q}(\pm 1)^{n_j}\psi_{n_1,\ldots,n_Q}(t) \\ &\quad \times\exp\left\{\frac{i}{\hbar}[Q(E_0-2|J|)t]\right\}. \end{aligned} \tag{B6}$$

As a result, we obtain the following pair of coupled discrete nonlinear field equations. The symmetric wave function $\{\phi_{n_1,\ldots,n_Q}(\tau)\}$ is coupled with the one-dimensional displacement field $\{y_n(\tau)\}$ [cf. Eqs. (58) and (59)]:[27]

$$i\frac{d}{d\tau}\phi_{n_1,\ldots,n_Q}=-D\left[\sum_{j=1}^{Q}(\phi_{n_1,\ldots,n_j-1,\ldots,n_Q}+\phi_{n_1,\ldots,n_j+1,\ldots,n_Q})-2Q\phi_{n_1,\ldots,n_Q}\right]+g\left[\sum_{j=1}^{Q}y_{n_j}\right]\phi_{n_1,\ldots,n_Q}\,, \tag{B7}$$

and

$$\frac{d^2}{d\tau^2}y_n=-y_n-Qg\sigma\sum_{n_1,\ldots,n_{Q-1}}|\phi_{n_1,\ldots,n_{Q-1},n}|^2\,. \tag{B8}$$

Here, the parameters are given by (60).

The corresponding discrete NLS equation, which follows from Eqs. (B7) and (B8) when the inertia term on the left-hand-side of Eq. (B8) is omitted, has the form

$$\begin{aligned} & i\frac{d}{d\tau}\phi_{n_1,\ldots,n_Q}+D\left[\sum_{j=1}^{Q}(\phi_{n_1,\ldots,n_j-1,\ldots,n_Q}+\phi_{n_1,\ldots,n_j+1,\ldots,n_Q})-2Q\phi_{n_1,\ldots,n_Q}\right] \\ &\qquad +Q\lambda\left[\sum_{j=1}^{Q}\sum_{n_1,\ldots,\tilde{n}_j,\ldots,n_Q}|\phi_{n_1,\ldots,n_Q}|^2\right]\phi_{n_1,\ldots,n_Q}=0\,, \end{aligned} \tag{B9}$$

where $\tilde{n}_j$ denotes the absence of the summation with respect to this index. Note that the corresponding generalization of the Ablowitz-Ladik equation, which admits the exact soliton solution in the discrete case, can be written as

$$\begin{aligned} & i\frac{d}{d\tau}\phi_{n_1,\ldots,n_Q}+D\left[\sum_{j=1}^{Q}(\phi_{n_1,\ldots,n_j-1,\ldots,n_Q}+\phi_{n_1,\ldots,n_j+1,\ldots,n_Q})-2Q\phi_{n_1,\ldots,n_Q}\right] \\ &\qquad +\frac{1}{2}Q\lambda\sum_{j=1}^{Q}\left[\sum_{n_1,\ldots,\check{n}_j,\ldots,n_Q}|\phi_{n_1,\ldots,n_Q}|^2\right](\phi_{n_1,\ldots,n_j-1,\ldots,n_Q}+\phi_{n_1,\ldots,n_j+1,\ldots,n_Q})=0\,. \end{aligned} \tag{B10}$$

The soliton solution of this equation has the following factorized form:

$$\phi_{n_1,\ldots,n_Q}(\tau)=\prod_{j=1}^{Q}\left[\frac{2D}{Q\lambda}\right]^{1/2}\sinh\mu_j\,\mathrm{sech}[\mu_j(n_j-s_j\tau)]\exp\{i[k_jn_j-2D(1-\cos k_j\cosh\mu_j)\tau]\}\,, \tag{B11}$$

where the velocities s_j and the wave numbers k_j are related through

$$s_j=2D\sin k_j(\sinh\mu_j/\mu_j)\,. \tag{B12}$$

The Q-particle wave function $\phi_{n_1,\ldots,n_Q}(\tau)$ is assumed to be normalized [see (B2)]. Therefore, from (B11) we get the condition

$$\sum_n \mathrm{sech}^2[\mu_j(n-s_j\tau)]=\frac{Q\lambda}{2D}\sinh^{-2}\mu_j\,. \tag{B13}$$

This condition is sufficient for (B11) to be a solution to Eq. (B10) in the case $Q\geq 2$. It may be considered as an equation to find μ_j. In the continuum limit (for small μ_j) one can easily find

$$\mu_j \simeq Q\lambda/4D \ . \tag{B14}$$

In the case $Q=1$ the soliton solution is well known, and there is no such constraint as (B13). We have

$$\phi_n(\tau)=(2d/\lambda)^{1/2}\sinh\mu\,\mathrm{sech}[\mu(n-s\tau)] \times\exp\{i[kn-2D(1-\cos k\cosh\mu)\tau]\}\ , \tag{B15}$$

with the free parameter μ as the inverse half-width of the soliton. However, we may still require the normalization condition to be fulfilled. In this case the soliton width becomes fixed and therefore $\mu \simeq \lambda/4D$, i.e., it depends on only the ratio of the nonlinear coupling λ to the dispersive term D.

Thus the form of the corresponding NLS equation describing the multiquanta dynamics of the intramolecular excitation is not the same as for one quantum. Since the energy 0.422 eV released during the ATP hydrolysis is a little more than twice the energy of an amide-*I* vibrational quantum (0.206 eV), the most interesting case for the multiquanta dynamical studies is $Q=2$. The two-quanta amide-*I* dynamics in a regular chain modeling crystalline acetanilide ACN has been numerically studied in Ref. 27. The results discussed there concern the two-soliton scattering and the formation of bisolitons.

---

*Permanent address: Institute for Theoretical Physics, Ukrainian Academy of Sciences, 252130 Kiev, Ukraine.

[1] A. S. Davydov and N. I. Kyslukha, Phys. Status Solidi B **59**, 465 (1973).

[2] D. Green, Science **181**, 583 (1973); Ann. N.Y. Acad. Sci. **227**, 6 (1974).

[3] Y. Toyazawa, Prog. Theor. Phys. **26**, 29 (1961).

[4] A. S. Davydov, Usp. Fiz. Nauk **138**, 603 (1982) [Sov. Phys. Usp. **25**, 898 (1982)].

[5] A. S. Davydov, *Solitons in Molecular Systems* (Reidel, Dordrecht, 1985).

[6] *Davydov's Soliton Revisited,* edited by P. L. Christiansen and A. C. Scott (Plenum, London, 1990).

[7] D. Y. Petrina and V. Z. Enol'skii, Dok. Akad. Nauk SSSR Ser. A, **8**, 759 (1976); A. S. Davydov and N. I. Kyslukha, Zh. Eksp. Teor. Fiz. **71**, 1090 (1976) [Sov. Phys. JETP **44**, 571 (1976)].

[8] J. M. Hyman, D. W. McLaughlin, and A. C. Scott, Physica D **3**, 23 (1981).

[9] A. C. Scott, Phys. Rev. A **26**, 578 (1982); Phys. Scr. **25**, 651 (1982); **29**, 279 (1984).

[10] L. MacNeil and A. C. Scott, Phys. Scr. **29**, 284 (1984).

[11] H. Bolterauer and R. D. Henkel, Phys. Scr. **T13**, 314 (1986).

[12] G. A. Velzen and J. A. Tjon, Phys. Lett. A **116**, 167 (1986).

[13] A. C. Scott, Phys. Rep. **217**, 1 (1992).

[14] L. Landau, Phys. Z. Sowjetunion **3**, 664 (1933).

[15] S. Pekar, J. Phys. (Moscow) **10**, 341 (1946); **10**, 347 (1946).

[16] T. D. Holstein, Ann. Phys. (N.Y.) **8**, 325 (1959); **8**, 343 (1959); L. A. Turkevich and T. D. Holstein, Phys. Rev. B **35**, 7474 (1987).

[17] G. Careri, U. Buontempo, F. Carta, E. Gratton, and A. C. Scott, Phys. Rev. Lett. **51**, 304 (1983); G. Careri, U. Buontempo, F. Galluzzi, A. C. Scott, E. Gratton, and E. Shyamsunder, Phys. Rev. B **30**, 4689 (1984); J. C. Eilbeck, P. S. Lomdahl, and A. C. Scott, *ibid.* **30**, 4703 (1984).

[18] P. W. Anderson, Phys. Rev. A **109**, A1492 (1958).

[19] J. G. Caputo, A. C. Newell, and M. Shelley, in *Stimulated Effects in Josephson Junctions,* edited by M. Russo and G. Costabile (World Scientific, Singapore, 1990).

[20] A. S. Davydov and A. V. Zolotaryuk, Phys. Lett. **94A**, 49 (1983); Phys. Scr. **28**, 249 (1983).

[21] A. S. Davydov and A. V. Zolotaryuk, Phys. Status Solidi B **115**, 115 (1983).

[22] A. A. Vakhnenko and Yu. B. Gaididei, Teor. Mat. Fiz. **68**, 350 (1986) [Sov. Theor. Math. Phys. **68**, 873 (1987)].

[23] A. V. Zolotaryuk and A. V. Savin, Physica D **46**, 295 (1990).

[24] M. J. Ablowitz and J. F. Ladik, Stud. Appl. Math. **55**, 213 (1976); J. Math. Phys. **17**, 1011 (1976); M. J. Ablowitz, Stud. Appl. Math. **58**, 17 (1978).

[25] K. Itoh and T. Shimanouchi, J. Mol. Spectrosc. **42**, 86 (1972).

[26] N. A. Nevskaya and Yu. N. Chirgadze, Biopolymers **15**, 637 (1976); **15**, 607 (1976).

[27] A. V. Savin and A. V. Zolotaryuk, in *Davydov's Soliton Revisited,* edited by P. L. Christiansen and A. C. Scott (Plenum, London, 1990), pp. 143-154.

[28] Yu. S. Kivshar in *Nonlinearity and Disorder,* edited by F. Kh. Abdullaev, A. R. Bishop, and St. Pnevmatikos (Springer, Berlin, 1991); F. Kh. Abdullaev and P. K. Khabibullaev, *Soliton Dynamics in Inhomogeneous Condensed Media* (FAN, Tashkent, 1986).

[29] P. Devillard and C. M. Souillard, J. Stat. Phys. **43**, 423 (1986); B. Doucot and R. Rammal, Europhys. Lett. **3**, 969 (1987); J. Phys. (Paris) **48**, 509 (1987).

[30] Yi Wan and C. M. Soukoulis, in *Disorder and Nonlinearity,* edited by A. R. Bishop, D. K. Campbell, and St. Pnevmatikos, Springer Proceedings in Physics, Vol. 39 (Springer, Berlin, 1989), pp. 27-37.

[31] A. V. Savin, Ukr. Fiz. Zh. **34**, 1300 (1989).

[32] L. S. Brizhyk and A. S. Davydov, Fiz. Nizk. Temp. **10**, 748 (1984); **10**, 358 (1984); A. S. Davydov and I. I. Ukrainsky, Can. J. Chem. **63**, 1899 (1985).

[33] D. Lj. Mirjanić, M. M. Marinković, G. Knežvić, and B. S. Tošić, Phys. Status Solidi B **121**, 589 (1984); A. V. Zolotaryuk, in *Physics of Many Particle Systems,* edited by A. S. Davydov (Naukova Dumka, Kiev, 1988), No. 13, pp. 40–52; W. C. Kerr and P. S. Lomdahl, in *Davydov's Soliton Revisited,* edited by P. L. Christiansen and A. C. Scott (Plenum, London, 1990), pp. 23–30.